



Whole-exome sequencing in cervical adenocarcinoma in mainland Chinese patients

Xinxin Zhang^{1,2,3#}, Jing Guo^{4#}, Yaping Cai⁴, Xiugui Sheng^{1,2}

¹Department of Gynecologic Oncology, Shandong Cancer Hospital and Institute, Shandong First Medical University and Shandong Academy of Medical Sciences, Jinan, China; ²Cancer Hospital of Chinese Academy of Medical Sciences, Shenzhen Center, Shenzhen, China; ³Cheeloo College of Medicine, Shandong University, Jinan, China; ⁴Department of Medical Oncology, Xiamen Key Laboratory of Antitumor Drug Transformation Research, The First Affiliated Hospital of Xiamen University, Xiamen, China

Contributions: (I) Conception and design: X Zhang, J Guo, X Sheng; (II) Administrative support: J Guo, X Sheng; (III) Provision of study materials or patients: X Zhang, X Sheng; (IV) Collection and assembly of data: X Zhang, J Guo; (V) Data analysis and interpretation: X Zhang, J Guo, Y Cai; (VI) Manuscript writing: All authors; (VII) Final approval of manuscript: All authors.

[#]These authors contributed equally to this work.

Correspondence to: Xiugui Sheng. National Cancer Center, National Clinical Research Center for Cancer and Cancer Hospital & Shenzhen Hospital, Chinese Academy of Medical Sciences and Peking Union Medical College, 113 Baohe Rd., Longgang Dist., Shenzhen, Guangdong, 518116, China. Email: shengxiugui@163.com.

Background: Cervical cancer is the most common gynecological malignancy worldwide. Adenocarcinoma is an important pathological type of cervical cancer. In recent years, the incidence of adenocarcinoma is rising in some countries and the prognosis of it remains poor. A precise description of the mutational landscape in cervical adenocarcinoma may provide insights into a better selection of treatments and improve prognosis.

Methods: In this study, we conducted whole-exome sequencing (WES) for cervical adenocarcinomas and matched blood samples from a cohort of 24 mainland Chinese patients. Additionally, the Human-Papilloma virus (HPV) infection statuses of these tumor samples were detected, and the genes that were enriched in both HPV positive and negative samples were also analyzed.

Results: The results of WES revealed the gene expression profile of cervical adenocarcinoma of women in mainland China and identified multiple genes/pathways, which are frequently mutated in these tumors, including the *PI3K-AKT* (*KRAS*, *PIK3CA* and *PTEN*), estrogen signaling (*KRAS*, *PIK3CA* and *GNAS*) and NK cell-mediated antibody-dependent cellular cytotoxicity pathways. Besides, seven patients had HPV infection, and the mutated genes in HPV-positive tumor tissues were relatively consistent, while the mutation profiles of HPV-negative tumor tissues were relatively scattered.

Conclusions: Taken together, these findings provide novel insights into the pathogenesis of cervical adenocarcinomas. They suggest the potential for individualized treatment of cervical adenocarcinoma according to genomic information.

Keywords: Cervical adenocarcinoma; whole-exome sequencing (WES); somatic mutations

Submitted Dec 23, 2019. Accepted for publication Sep 20, 2020.

doi: 10.21037/tcr-19-2930

View this article at: <http://dx.doi.org/10.21037/tcr-19-2930>

Introduction

With the promotion and popularization of cervical cancer screening, the global incidence of cervical cancer has increased in recent years (1,2). Cervical cancer markedly contributes to the cancer burden in China, with

110,000 new cases and 34,000 related deaths in 2018 (3). Among the different pathological types of cervical cancer, adenocarcinoma is second only to squamous cell carcinoma, accounting for 10–25% of cervical cancer cases. Furthermore, adenocarcinoma of the cervix is an

aggressive tumor and can progress to lymph node or distant metastases at an early stage. With poor sensitivity to the radiation therapy, cervical adenocarcinoma is considered by most researchers to have a poor prognosis. Even though the pathogenesis of cervical cancer has been extensively studied, the exact mechanisms of carcinogenesis remain unclear (4). It is widely believed that persistent infection with oncogenic types of human papillomavirus (HPV), especially HPV18, represents the most important risk factor for the development of cervical adenocarcinoma (5,6). Nevertheless, HPV infection alone is not sufficient for neoplastic transformation, and other genetic events, independent or in combination with HPV infection, are required (7). Therefore, a deeper understanding of the molecular basis of cervical adenocarcinoma, and the development of new and more effective therapy, remain unmet medical needs.

In the current study, we sequenced the exomes of a large cohort of fresh-frozen cervical adenocarcinoma tissue, and determined the gene expression profile of cervical adenocarcinoma of women in mainland China. The results identified alterations in multiple genes of the *PIK3CA/AKT/mTOR*, estrogen signaling, and NK (natural killer) cell-mediated antibody-dependent cellular cytotoxicity pathways.

We present the following article in accordance with the MDAR checklist (available at <http://dx.doi.org/10.21037/tcr-19-2930>).

Methods

Clinical material

Pretreatment tumor tissue and matched blood samples from 24 mainland Chinese patients with cervical adenocarcinoma were collected from the Department of Gynecologic Oncology, Shandong Cancer Hospital, from January 2018 to January 2019. The study was conducted in accordance with the Declaration of Helsinki (as revised in 2013). The study was approved by Ethics Committee of Shandong Cancer Hospital (No.: SDSZLYY20190315), and individual consent for this retrospective analysis was waived. All hematoxylin-eosin-stained sections of tumor tissues were reviewed by a pathologist to confirm the histological type. Genomic DNA isolated from peripheral blood was obtained from each patient as a corresponding control.

Whole exome-sequencing (WES)

DNA extraction and quality control

Genomic DNA was extracted from tumor samples and matched blood cells using the DNA Mini Kit (Qiagen, Hilden, Germany) according to the manufacturer's instructions. Careful quality control steps were applied to ensure that high-quality DNA samples were obtained. These steps included agarose gel electrophoresis tests to confirm that there was no obvious DNA degradation or RNA contamination, testing of DNA fragment sizes (Agilent Technologies, Santa Clara, CA, USA), and testing of OD values using a NanoDrop (Thermo Scientific, MA, USA).

Library construction, target capturing and sequencing

Matched tumor and blood cell samples from 24 cervical cancer patients were subjected to exome sequencing using the Illumina platform. Exome capture and paired-end sequencing of DNA was performed using the Paired-End Sample Preparation Kit (Illumina, San Diego, CA, USA) followed by in-solution capture of genomic DNA using the SureSelect Human All Exon V6 Kit (Agilent Technologies, Santa Clara CA, USA), targeting 37 Mb of exonic sequence. For each sample, captured DNA was sequenced by multiplexed paired-end sequencing using 2 pools of samples on the Illumina HiSeq 4000 platform (Illumina, San Diego, CA, USA), which yielded 10 Gb of reads with a read length of 150 bp.

Identification of somatic mutation sites and downstream analysis

Raw reads were filtered using fastp (v0.19), and the resulting clean reads were mapped to the human reference genome version 38 (hg38) using bwa (v0.7). Then, GATK (v4.1) was used to call somatic variants for each sample pair. Somatic mutations were filtered by criterion of frequency <0.01 in 1,000 Genomes, and nonsynonymous mutations in coding regions. These high-quality somatic mutation sites were annotated using ANNOVAR (v201804) with the refGene, 1,000 Genomes, dbSNP and COSMIC databases. Sites matching relevant records in COSMIC were used for further analysis. The flowchart of result analysis is indicated in [Figure S1](#). The PATHVIEW platform was used to visualize tumor pathways related to the corresponding genes.

HPV infection status and integrating locus

HPV genotypes for each sample were determined by polymerase chain reaction (PCR) and reverse dot hybridization. Fifteen high-risk HPV types [16, 18, 31, 33, 35, 39, 45, 51, 52, 56, 58, 59, 68, 73, 82], three likely high-risk HPV types [26, 53, 66], and ten low-risk HPV types [6, 11, 40, 42, 43, 44, 54, 61, 81, 83] were examined. In the PCR step, 20 μ L of extracted genomic DNA was centrifuged at 6,000 rpm for 5 s and then amplified with the following thermal profile: 3 min of preparation at 50 °C; 15 min of activation at 95 °C; 40 cycles of 40 s of denaturation at 94 °C, 40 s of annealing at 55 °C, and 40 s of extension at 72 °C, and a 7-min final extension at 72 °C. After removal from the thermal cycler, samples were stored at 4 °C for more than 2 min. In the hybridization step, the corresponding HPV nylon membrane strip, 4 mL of hybrid solution I and 40 μ L of the PCR products were mixed in a well and reacted in a shaking (100 rpm) water bath at 42 °C for 1 h. Following hybridization, the strips were briefly rinsed and mixed with 3 mL of prewarmed (42 °C) solution II in another well, and the trays were incubated in a shaking water bath at 42 °C for 10 min. After the stringent wash, the buffer was removed, 6 mL of prewarmed (42 °C) solution II was added to each well, and the tray was placed in a shaking water bath at 42 °C for 10 min. After the final wash, the buffer was removed, and the strips were rinsed and photographed within 2 h of color development in a sealed plastic bag in the dark. HPV genotyping results were obtained by scanning the photographed strips.

To detect the genomic integrating locus for each HPV-positive sample, WES read pairs with one segment mapped and the mate unmapped were filtered using Samtools. The unmapped mate sequences were used as BLAST queries to search for homologous fragments in 180 HPV genomes obtained from the GenBank database. Hits with E-values lower than 10⁻¹⁰ and query coverage more than 80% were regarded as positive hits, and the positions of their mate reads were regarded as putative HPV integrating loci.

Statistical analysis

R 3.6.0 statistical software was used for data analysis. Statistical analysis was performed with Wilcoxon Rank Sum Tests and Fisher's Exact Tests. $P < 0.05$ was considered statistically significant.

Results

Clinical material

Tumor tissue and matched blood samples from 24 mainland Chinese women with cervical adenocarcinoma [9 stage I, 6 stage II, 8 stage III, and 1 stage IV, according to the International Federation of Gynecology and Obstetrics (FIGO) staging system] aged between 25 and 71 years at the time of diagnosis were included in the present study. Of the 24 patients, 7 had HPV infection, and among these patients, 3 were positive for HPV16, 3 were positive for HPV18, and 1 was positive for HPV16 and HPV18. In 3 of the patients, the HPV was integrated into the genome. The demographic details of these patients are summarized in *Table 1*.

Quality control and comparison results

According to the description in the Materials and Methods, the quality control results of the 24 cervical adenocarcinomas and matched blood cell samples met the requirements. Similarly, the alignment of the above specimens also met the requirements, indicating that these samples were not contaminated (*Figure S2*).

Exome sequencing and somatic variations

The peripheral blood control of each patient was used to filter out the germline variations, and further quality filtering led to the detection of 23,139 somatic variations falling within coding regions, of which 19,954 (86.2%) were nonsynonymous single-nucleotide variants (SNVs), 1,742 (7.5%) were stop-gain mutations, and the remaining variations were mainly frameshift mutations and non-frameshift variations in the 24 tumors (*Figure 1A*). Further analysis found that the mutation count of HPV-positive patients was far lower than that of the HPV-negative cases in stage I; however, there was only a slight difference in mutation count between HPV-positive and HPV-negative patients in stage II and III patients (*Figure 1B,C,D*). Venn diagram was used to compare the mutated genes among these patients in each stage (*Figure 2*).

Gene mutation frequency in patients

Figure 3A indicates that 70 genes were found to be mutated

Table 1 Demographic details of the 24 patients included in this study

NO	Histology	FIGO stage	Age (years)	HPV type	Integration locus
T1	Adenocarcinoma	IIB	62	HPV18	Unknown
T2	Adenocarcinoma	IB1	50	Not detected	–
T3	Adenocarcinoma	IIB	41	Not detected	–
T4	Adenocarcinoma	IB2	56	Not detected	–
T6	Adenocarcinoma	IIB	62	HPV18	16q21
T8	Adenocarcinoma	IB	38	Not detected	–
T9	Adenocarcinoma	IIA	31	Not detected	–
T12	Adenocarcinoma	IIIA	66	Not detected	–
T13	Adenocarcinoma	IIIB	58	Not detected	–
T14	Adenocarcinoma	IB	43	Not detected	–
T16	Adenocarcinoma	IB	41	Not detected	–
T18	Adenocarcinoma	IIIB	71	Not detected	–
T23	Adenocarcinoma	IB	34	HPV16, HPV18	1p36.12, 1p32.3, 10q22.2, 12p13.31, 17p12, 17q12, 17q22, 3p21.1, 6p25.2, 9q21.12, 9q22.33, 9q34.13,
T26	Adenocarcinoma	IV	66	Not detected	–
T27	Adenocarcinoma	IIIB	62	HPV16	Unknown
T28	Adenocarcinoma	IB	25	Not detected	–
T30	Adenocarcinoma	IIIB	61	Not detected	–
T32	Adenocarcinoma	IIIB	47	Not detected	–
T33	Adenocarcinoma	IIIB	66	HPV16	Unknown
T34	Adenocarcinoma	IB1	43	HPV18	Unknown
T36	Adenocarcinoma	IIB	71	Not detected	–
T37	Adenocarcinoma	IIIB	50	HPV16	12q22, 18q21.33
T39	Adenosquamous	IB1	49	Not detected	–
T41	Adenocarcinoma	IIB	30	Not detected	–

FIGO, International Federation of Gynecology and Obstetrics; HPV, human papillomavirus.

in at least 3 tumors. *Figure 3B* shows that the mutated genes in HPV-positive tumor tissues were relatively consistent, with 17 genes enriched in these samples (*Table 2*), while the mutation profiles of HPV-negative tumor tissues were relatively scattered, with only 1 gene, *HUWE1*, enriched in HPV-negative tumor tissue (*Table 3*). The top 10 most frequently mutated genes among these tumor sample are summarized in *Table 4*.

Somatic mutations associated with cervical cancer

The Catalogue of Somatic Mutations in Cancer (COSMIC) database was used to annotate the variation sites of each sample, and the variation of cervical cancer was screened by linking each mutation site. Screening results showed that 8 sites in 6 genes (*KRAS*, *NRAS*, *PIK3CA*, *PTEN*, *GNAS*, *HLA-A*) were associated with cervical adenocarcinoma

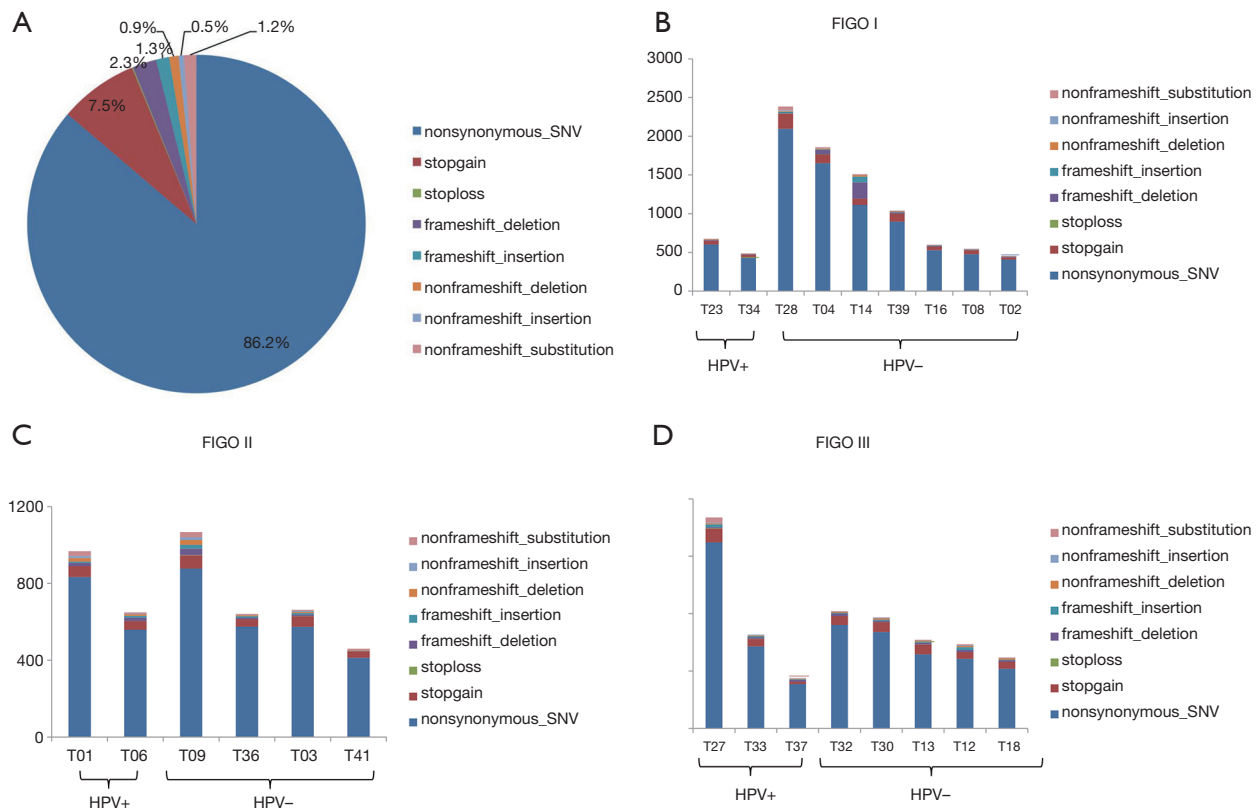


Figure 1 Somatic mutations in cervical adenocarcinoma. (A) Somatic mutation types in tumors of 24 cervical adenocarcinoma patients. (B-D) Somatic mutation counts of HPV-negative and HPV16-positive patients with stage I, II, and III cervical adenocarcinoma. FIGO, International Federation of Gynecology and Obstetrics; HPV, human papillomavirus; SNV, single-nucleotide variants.

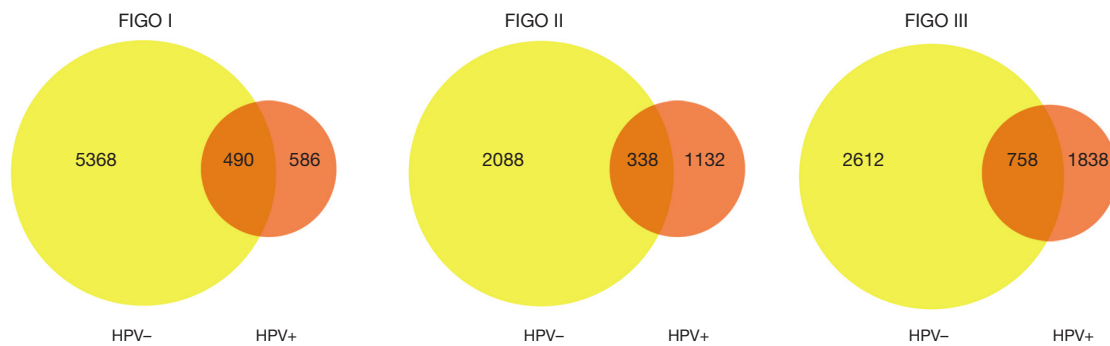


Figure 2 Venn diagram of somatically mutated genes between HPV negative and HPV positive patients with stage I, II and III cervical adenocarcinoma. FIGO, International Federation of Gynecology and Obstetrics; HPV, human papillomavirus.

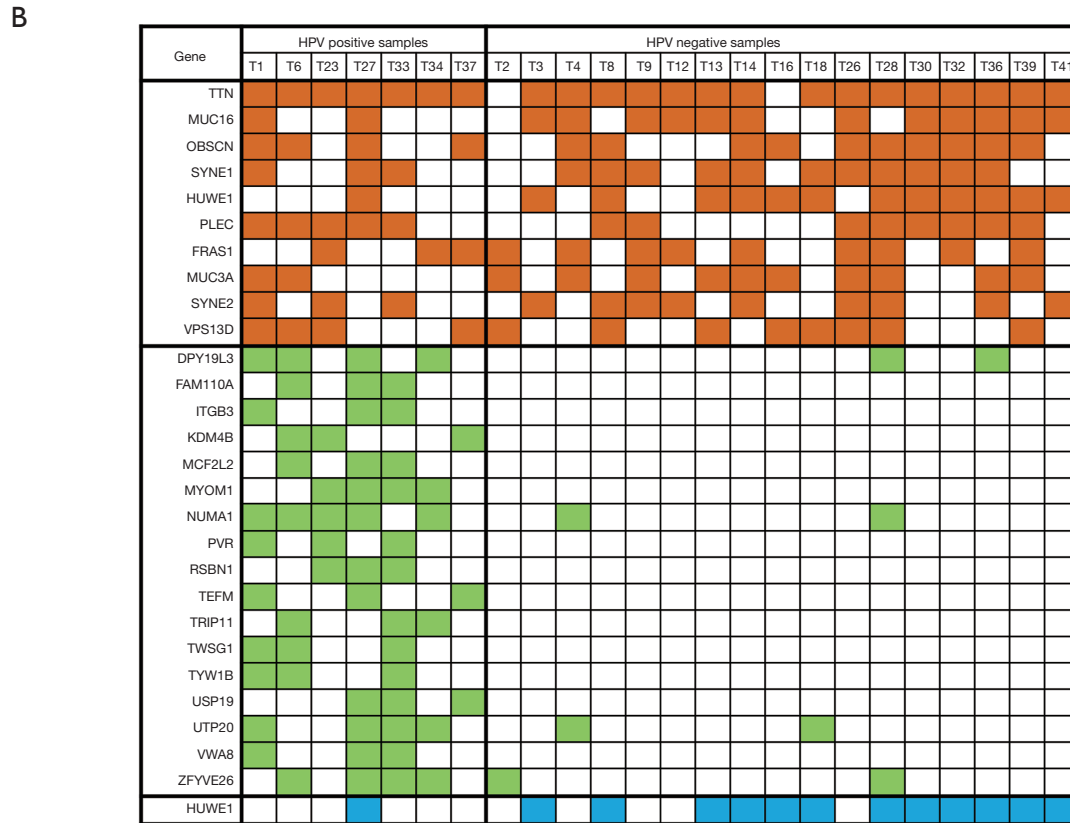
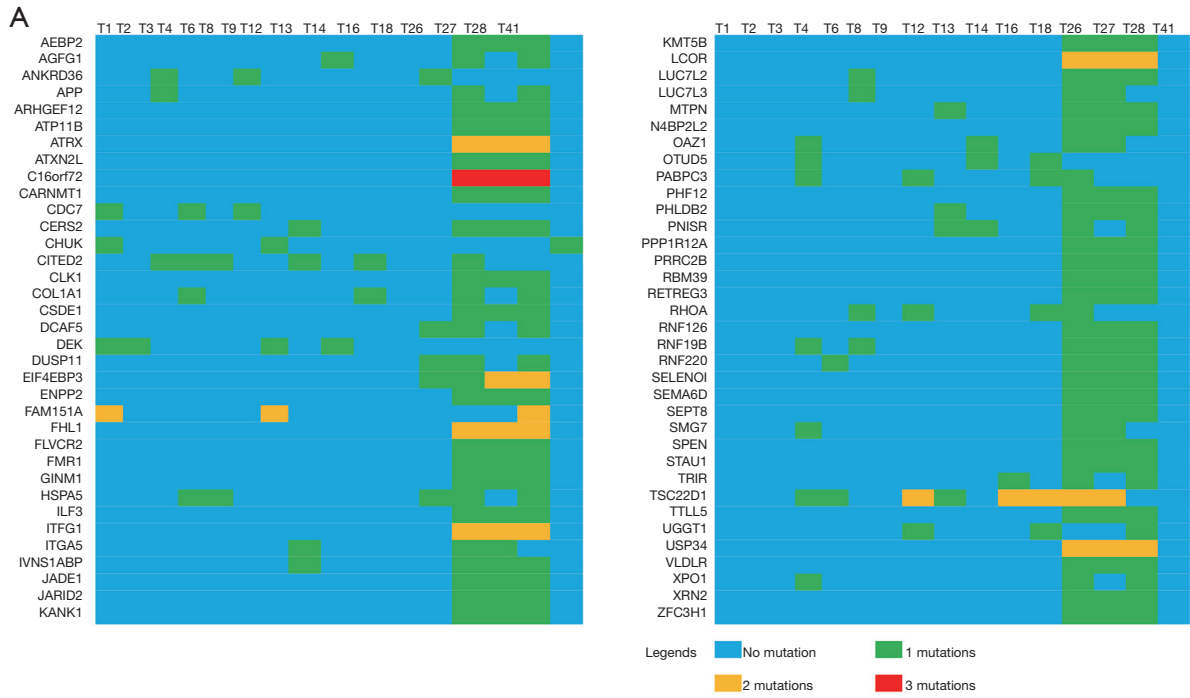


Figure 3 Gene mutation frequency in patients. (A) Heat map of frequently mutated genes. In all, 70 genes were found to be mutated in at least 3 tumors. (B) The most mutated genes in all the samples (orange), genes with high mutation rates in HPV-positive tissues (green), and genes with high mutation rates in HPV negative tissues (blue).

Table 2 Genes enriched in HPV-positive samples

Gene	HPV positive		HPV negative		P value
	Samples with mutations	Samples without mutations	Samples with mutations	Samples without mutations	
<i>DPY19L3</i>	4	3	2	15	0.038
<i>FAM110A</i>	3	4	0	17	0.017
<i>ITGB3</i>	3	4	0	17	0.017
<i>KDM4B</i>	3	4	0	17	0.017
<i>MCF2L2</i>	3	4	0	17	0.017
<i>MYOM1</i>	4	3	0	17	0.003
<i>NUMA1</i>	5	2	2	15	0.009
<i>PVR</i>	3	4	0	17	0.017
<i>RSBN1</i>	3	4	0	17	0.017
<i>TEFM</i>	3	4	0	17	0.017
<i>TRIP11</i>	3	4	0	17	0.017
<i>TWSG1</i>	3	4	0	17	0.017
<i>TYW1B</i>	3	4	0	17	0.017
<i>USP19</i>	3	4	0	17	0.017
<i>UTP20</i>	4	3	2	15	0.038
<i>VWA8</i>	3	4	0	17	0.017
<i>ZFYVE26</i>	4	3	2	15	0.038

HPV, human papillomavirus; *DPY19L3*, dpy-19 like C-mannosyltransferase 3; *FAM110A*, family with sequence similarity 110 member A; *ITGB3*, integrin subunit beta 3; *KDM4B*, lysine demethylase 4B; *MCF2L2*, MCF.2 cell line derived transforming sequence-like 2; *MYOM1*, myomesin 1; *NUMA1*, nuclear mitotic apparatus protein 1; *PVR*, PVR cell adhesion molecule; *RSBN1*, round spermatid basic protein 1; *TEFM*, transcription elongation factor, mitochondrial; *TRIP11*, thyroid hormone receptor interactor 11; *TWSG1*, twisted gastrulation BMP signaling modulator 1; *TYW1B*, tRNA-yW synthesizing protein 1 homolog B; *USP19*, ubiquitin specific peptidase 19; *UTP20*, UTP20 small subunit processome component; *VWA8*, von Willebrand factor A domain containing 8; *ZFYVE26*, zinc finger FYVE-type containing 26.

Table 3 Gene enriched in HPV-negative samples

Gene	HPV positive		HPV negative		P value
	Samples with mutations	Samples without mutations	Samples with mutations	Samples without mutations	
<i>HUWE1</i>	1	6	12	5	0.018

HUWE1, *HECT*, *UBA* and *WWE* domain containing E3 ubiquitin protein ligase 1. HPV, human papillomavirus.

(Table 5). Further analysis showed that these six were mainly involved in the *PIK3CA/AKT/mTOR* pathway, estrogen signaling, and natural killer (NK) cell-mediated antibody-dependent cellular cytotoxicity (Figure 4). Therefore, these signaling pathways are the major alterations in cervical adenocarcinoma.

Discussion

This study conducted whole-exome sequencing (WES) of fresh-frozen tumors from a cohort of mainland Chinese patients with cervical adenocarcinoma. The results revealed a heterogeneous mutation spectrum, and identified some frequently altered genes, including *KRAS/NRAS*, *PIK3CA/*

Table 4 The top 10 most mutated genes in all samples

Gene	Samples with mutations	Proportion
<i>TTN</i>	22	91.67%
<i>MUC16</i>	14	58.33%
<i>OBSCN</i>	14	58.33%
<i>SYNE1</i>	14	58.33%
<i>HUWE1</i>	13	54.17%
<i>PLEC</i>	13	54.17%
<i>FRAS1</i>	12	50.00%
<i>MUC3A</i>	12	50.00%
<i>SYNE2</i>	12	50.00%
<i>VPS13D</i>	12	50.00%

TTN, titin; *MUC16*, mucin 16, cell surface associated; *OBSCN*, obscurin, cytoskeletal calmodulin and titin-interacting RhoGEF; *SYNE1*, spectrin repeat containing nuclear envelope protein 1; *HUWE1*, HECT, UBA and WWE domain containing E3 ubiquitin protein ligase 1. *PLEC*, plectin; *FRAS1*, Fraser extracellular matrix complex subunit 1; *MUC3A*, mucin 3A, cell surface associated; *SYNE2*, spectrin repeat containing nuclear envelope protein 2; *VPS13D*, vacuolar protein sorting 13 homolog D.

PTEN, *GNAS*, and *HLA-A*. The mutation rates of these genes were 19.0%, 14.3%, 9.5%, and 4.8%, respectively. *KRAS* has been confirmed as the most commonly mutated oncogene, and approximately 30% of human malignancies could be detected with somatic mutations (8-12). *KRAS* was also a frequently altered gene in this group of tumors, with nonsynonymous SNVs detected in 3 tumors (14.3%, 3/21), and this result was in accordance with previous studies (13,14). *KRAS* encodes a protein that acts as a GTPase and plays an important role in regulating cell proliferation, differentiation, and survival (15). To date, *KRAS* proteins have not yielded any effective targeted therapies due to their complex structure. However, the status of *KRAS* mutations helps the selection of patients who are sensitive to the targeted treatments. For example, anti-epidermal growth factor receptor (*EGFR*) antibodies are more effective in patients with *RAS* wild-type metastatic colorectal cancer (CRC) than in patients with mutant *RAS* (16), while the combination of an *MEK* inhibitor and *FGFR1* inhibitor induces tumor cell death in *KRAS*-mutant lung cancer cells (9).

The *PI3K/AKT* pathway has core effects in various cellular responses, including cell proliferation, migration,

Table 5 Variations data related to the cervical adenocarcinoma detect by whole exome sequencing

Chromosome	Location	Gene	Variation type	Variation	Rs No.	Sample mutation abundance	COSMIC ID	FATHMM evaluation
chr20	58909365	<i>GNAS</i>	Nonsynonymous SNV	c.2530C>T p.R844C	rs11554273	T33:16.6%; T37:29.6%	COSM123397; COSM27887	Pathopoiesis
chr6	29942967	<i>HLA-A</i>	Stop gain	c.284C>G p.S95		T8:10.6%	COSM4847247; COSM4847248	Neutrality
chr12	25245350	<i>KRAS</i>	Nonsynonymous SNV	c.35G>A p.G12D	rs121913529	T18:6.4%	COSM1135366; COSM521	Pathopoiesis
chr12	25245347	<i>KRAS</i>	Nonsynonymous SNV	c.38G>A p.G13D	rs112445441	T36:25.8%; T4:27.2%	COSM532; COSM1140132	Pathopoiesis
chr1	114713908	<i>NRAS</i>	Nonsynonymous SNV	c.182A>G p.Q61R	rs11554290	T14:21.9%	COSM584	Pathopoiesis
chr3	179234297	<i>PIK3CA</i>	Nonsynonymous SNV	c.3140A>G p.H1047R	rs121913279	T33:10.1%	COSM94986; COSM775	Pathopoiesis
chr10	87933147	<i>PTEN</i>	Stop gain	c.388C>T p.R130	rs121909224	T14:24.3%	COSM5152	Pathopoiesis
chr10	87957915	<i>PTEN</i>	Stop gain	c.697C>T p.R233	rs121909219	T4:49.6%	COSM5154	Pathopoiesis

COSMIC, Catalogue of Somatic Mutations In Cancer; SNV, single-nucleotide variants; FATHMM, Functional Analysis Through Hidden Markov Models; *GNAS*, *GNAS* complex locus; *HLA-A*, major histocompatibility complex, class I, A; *KRAS*, *KRAS* proto-oncogene, GTPase; *NRAS*, *NRAS* proto-oncogene, GTPase; *PIK3CA*, phosphatidylinositol-4,5-bisphosphate 3-kinase catalytic subunit alpha; *PTEN*, phosphatase and tensin homolog.

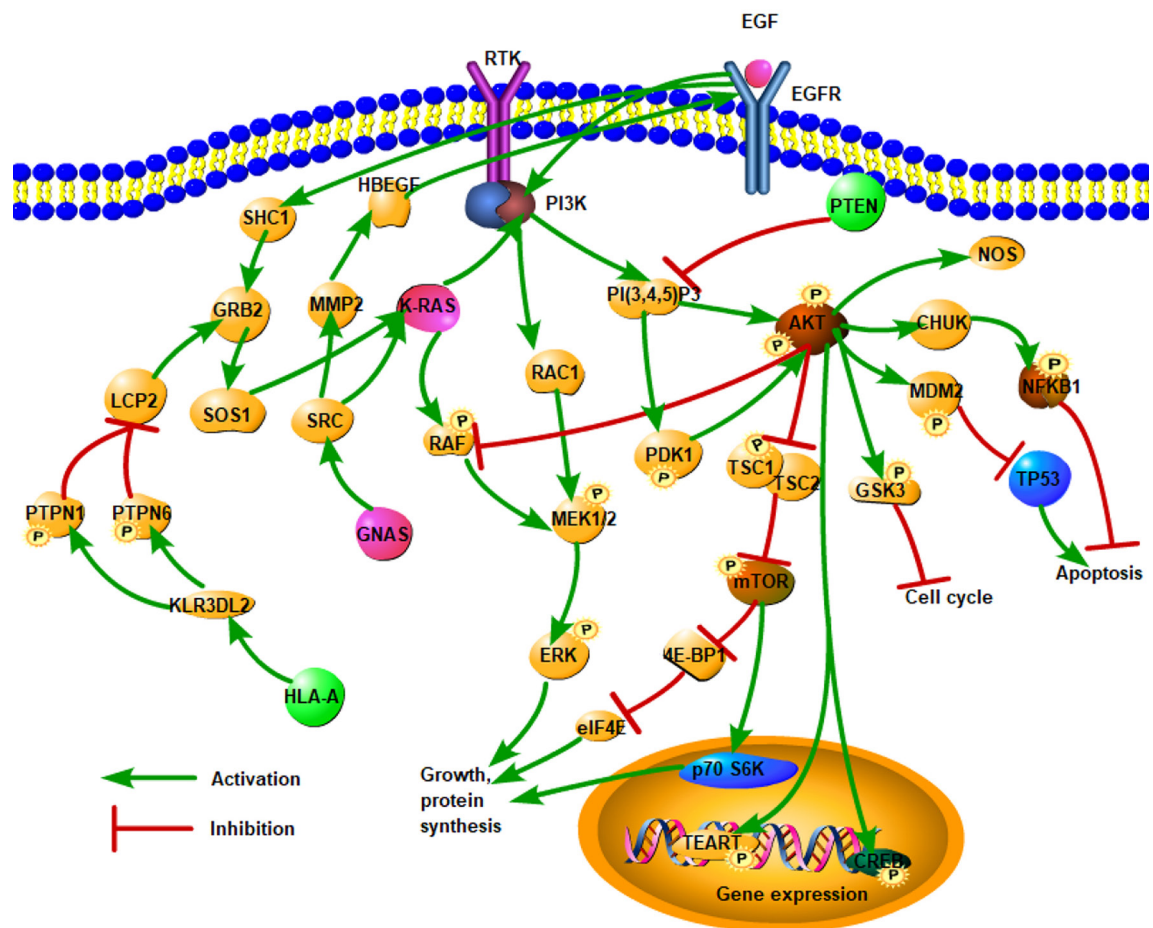


Figure 4 Mutant genes related to cervical adenocarcinoma detected by whole-exome sequencing and the associated signaling pathways, including the PI3K-AKT (KRAS, PIK3CA and PTEN), estrogen signaling (KRAS, PIK3CA and GNAS), and NK cell-mediated antibody-dependent cellular cytotoxicity pathways.

and metabolism (17). *PIK3CA* and *PTEN* have been established as the main genes involved in alterations in this signaling cascade (18). Our results indicated that 4.5% of tumor samples harbored nonsynonymous SNVs of *PIK3CA*, and 9.1% harbored stop-gain mutants of the *PTEN* gene. The recently reported mutations in *ERBB2* were not detected in this study, possibly because of the low sample size. These results suggest the involvement of this signaling cascade in cervical adenocarcinoma. Moreover, preclinical data showed that patients with *PIK3CA* mutations exhibited a high response rate to *PI3K/AKT/mTOR* pathway inhibitors (19). Similarly, loss of enzyme activity induced by somatic missense mutation of *PTEN* could be predictive of the efficacy of the aforementioned therapy. These findings indicate that a subgroup of cervical adenocarcinomas might

greatly benefit from *PI3K/AKT/mTOR* axis inhibitors.

Two tumors harbored nonsynonymous SNVs in *GNAS*. Previous studies have shown that *GNAS* mutations are detected in intraductal mucinous carcinoma of the pancreas and in mucinous endocervical adenocarcinoma. Furthermore, activation of *GNAS* via mutation has been found to induce high adenylyl cyclase activity and improve the level of adenosine 3',5'-monophosphate (cAMP) (20-22). The GPCR pathway is a known primary target for pharmaceutical research, and a medicine targeting GPCRs has been indicated to inhibit the malignant phenotypes of various human tumor cells. The results of this study provide potential treatment options for patients with cervical adenocarcinoma.

To our knowledge, this is the first study in which WES

has been applied to define the mutational landscape of cervical adenocarcinoma in mainland Chinese patients, and the results identified multiple genes/pathways that are frequently mutated in these tumors. These findings will help guide further study and targeted therapies against this cancer worldwide.

Acknowledgments

Funding: This work was supported by Sanming Project of Medicine in Shenzhen (No. SZSM201812075), Taishan Scholars (No. ts201511073), and Special fund for scientific talents of the First Affiliated Hospital of Xiamen University (No. ZLYY201906), National Natural Science Foundation of China (NSFC81672591), National Natural Science Foundation of Fujian Province (2020J05308). The authors are grateful to all the patients included in this study.

Footnote

Reporting Checklist: The authors have completed the MDAR checklist. Available at <http://dx.doi.org/10.21037/tcr-19-2930>

Data Sharing Statement: Available at <http://dx.doi.org/10.21037/tcr-19-2930>

Conflicts of Interest: All authors have completed the ICMJE uniform disclosure form (available at <http://dx.doi.org/10.21037/tcr-19-2930>). The authors have no conflicts of interest to declare.

Ethical Statement: The authors are accountable for all aspects of the work in ensuring that questions related to the accuracy or integrity of any part of the work are appropriately investigated and resolved. The study was conducted in accordance with the Declaration of Helsinki (as revised in 2013). The study was approved by Ethics Committee of Shandong Cancer Hospital (No.: SDSZLYY20190315), and individual consent for this retrospective analysis was waived.

Open Access Statement: This is an Open Access article distributed in accordance with the Creative Commons Attribution-NonCommercial-NoDerivs 4.0 International License (CC BY-NC-ND 4.0), which permits the non-commercial replication and distribution of the article with the strict proviso that no changes or edits are made and the

original work is properly cited (including links to both the formal publication through the relevant DOI and the license). See: <https://creativecommons.org/licenses/by-nc-nd/4.0/>.

References

1. Adegoke O, Kulasingam S, Virnig B. Cervical cancer trends in the United States: a 35-year population-based analysis. *J Womens Health (Larchmt)* 2012;21:1031-7.
2. Guo J, Zhang Y, Chen X, et al. Surgical and Oncologic Outcomes of Radical Abdominal Trachelectomy Versus Hysterectomy for Stage IA2-IB1 Cervical Cancer. *J Minim Invasive Gynecol* 2019;26:484-91.
3. Bray F, Ferlay J, Soerjomataram I, et al. Global cancer statistics 2018: GLOBOCAN estimates of incidence and mortality worldwide for 36 cancers in 185 countries. *CA Cancer J Clin* 2018;68:394-424.
4. Gupta SM, Mania-Pramanik J. Molecular mechanisms in progression of HPV-associated cervical carcinogenesis. *J Biomed Sci* 2019;26:28.
5. International Agency for Research on Cancer, World Health Organization. WHO Classification of Tumours of Female Reproductive Organs Lyon, France: International Agency for Research on Cancer 2014.
6. Bosch FX, Lorincz A, Muñoz N, et al. The causal relation between human papillomavirus and cervical cancer. *J Clin Pathol* 2002;55:244-65.
7. Wang SS, Hildesheim A. Chapter 5: Viral and host factors in human papillomavirus persistence and progression. *J Natl Cancer Inst Monogr* 2003;(31):35-40.
8. Xiang L, Li J, Jiang W, et al. Comprehensive analysis of targetable oncogenic mutations in Chinese cervical cancers. *Oncotarget* 2015;6:4968-75.
9. Manchado E, Weissmueller S, Morris JP 4th, et al. A combinatorial strategy for treating KRAS-mutant lung cancer. *Nature* 2016;534:647-51.
10. Wu CS, Wu SY, Chen HC, et al. Curcumin functions as a MEK inhibitor to induce a synthetic lethal effect on KRAS mutant colorectal cancer cells receiving targeted drug regorafenib. *J Nutr Biochem* 2019;74:108227.
11. Kandath C, Schultz N, Cherniack AD, et al. Integrated genomic characterization of endometrial carcinoma. *Nature* 2013;497:67-73.
12. Pylayeva-Gupta Y, Grabocka E, Bar-Sagi D. RAS oncogenes: weaving a tumorigenic web. *Nat Rev Cancer* 2011;11:761-74.
13. Wright AA, Howitt BE, Myers AP, et al. Oncogenic mutations in cervical cancer: genomic differences between

- adenocarcinomas and squamous cell carcinomas of the cervix. *Cancer* 2013;119:3776-83.
14. Kang S, Kim HS, Seo SS, et al. Inverse correlation between RASSF1A hypermethylation, KRAS and BRAF mutations in cervical adenocarcinoma. *Gynecol Oncol* 2007;105:662-6.
 15. Adjei AA. Blocking oncogenic Ras signaling for cancer therapy. *J Natl Cancer Inst* 2001;93:1062-74.
 16. Adelstein BA, Dobbins TA, Harris CA, et al. A systematic review and meta-analysis of KRAS status as the determinant of response to anti-EGFR antibodies and the impact of partner chemotherapy in metastatic colorectal cancer. *Eur J Cancer* 2011;47:1343-54.
 17. Hanker AB, Kaklamani V, Arteaga CL. Challenges for the Clinical Development of PI3K Inhibitors: Strategies to Improve Their Impact in Solid Tumors. *Cancer Discov* 2019;9:482-91.
 18. Millis SZ, Ikeda S, Reddy S, et al. Landscape of Phosphatidylinositol-3-Kinase Pathway Alterations Across 19 784 Diverse Solid Tumors. *JAMA Oncol* 2016;2:1565-73.
 19. Janku F, Tsimberidou AM, Garrido-Laguna I, et al. PIK3CA mutations in patients with advanced cancers treated with PI3K/AKT/mTOR axis inhibitors. *Mol Cancer Ther* 2011;10:558-65.
 20. Matsubara A, Sekine S, Ogawa R, et al. Lobular endocervical glandular hyperplasia is a neoplastic entity with frequent activating GNAS mutations. *Am J Surg Pathol* 2014;38:370-6.
 21. Wu J, Matthaei H, Maitra A, et al. Recurrent GNAS mutations define an unexpected pathway for pancreatic cyst development. *Sci Transl Med* 2011;3:92ra66.
 22. Freda PU, Chung WK, Matsuoka N, et al. Analysis of GNAS mutations in 60 growth hormone secreting pituitary tumors: correlation with clinical and pathological characteristics and surgical outcome based on highly sensitive GH and IGF-I criteria for remission. *Pituitary* 2007;10:275-82.

Cite this article as: Zhang X, Guo J, Cai Y, Sheng X. Whole-exome sequencing in cervical adenocarcinoma in mainland Chinese patients. *Transl Cancer Res* 2020;9(11):6889-6899. doi: 10.21037/tcr-19-2930